ACS APPLIED MATERIALS & INTERFACES

Research Article

www.acsami.org

Acceptor–Donor–Acceptor Small Molecules Based on Indacenodithiophene for Efficient Organic Solar Cells

Huitao Bai,[†,‡] Yifan Wang,[†,‡] Pei Cheng,[†,‡] Yongfang Li,[†] Daoben Zhu,[†] and Xiaowei Zhan*[,§]

[†]Beijing National Laboratory for Molecular Sciences, CAS Key Laboratory of Organic Solids, Institute of Chemistry, Chinese Academy of Sciences, Beijing 100190, China

[§]Department of Materials Science and Engineering, College of Engineering, Peking University, Beijing 100871, China

[‡]University of Chinese Academy of Sciences, Beijing 100049, China

Supporting Information

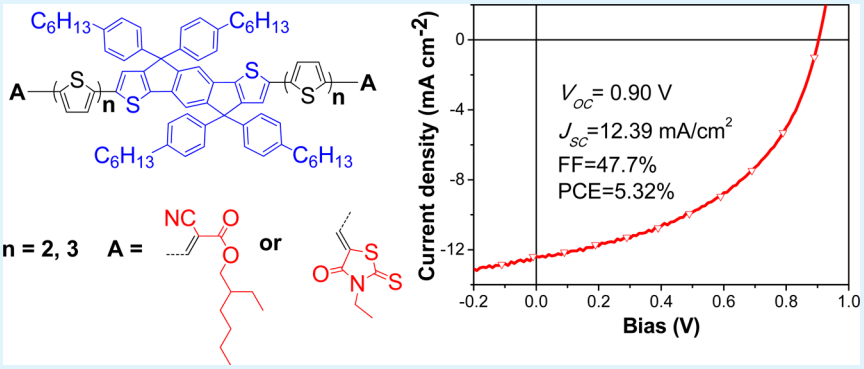

ABSTRACT: Four A-D-A type small molecules using 4,4,9,9-tetrakis(4-hexylphenyl)- indaceno[1,2-b:5,6-b′]dithiophene as central building block, bithiophene or terthiophene as π-bridges, alkyl cyanoacetate or rhodanine as end acceptor groups were synthesized and investigated as electron donors in solution-processed organic solar cells (OSCs). These molecules showed excellent thermal stability with decomposition temperatures over 360 °C, relatively low HOMO levels of −5.18 to −5.22 eV, and strong optical absorption from 350 to 670 nm with high molar extinction coefficient of 1.1×10^5 to 1.6×10^5 M^{-1} cm^{-1} in chloroform solution. OSCs based on blends of these molecules and $PC_{71}BM$ achieved average power conversion efficiencies of 2.32 to 5.09% (the best 5.32%) after thermal annealing. The effects of thiophene bridge length and end acceptor groups on absorption, energy level, charge transport, morphology, and photovoltaic properties of the molecules were investigated.

KEYWORDS: *small molecule solar cells, indacenodithiophene, alkyl cyanoacetate, rhodanine*

1. INTRODUCTION

Bulk heterojunction (BHJ) organic solar cells (OSCs) have attracted much attention because of their advantages of solution processability, low cost, light weight, flexibility, and potential application in large-area devices.[1−4] Over the last decades, by optimizing the polymer structure and device architecture, polymer solar cells made great progress in achieving high power conversion efficiencies (PCEs). Recently, the encouraging PCE of 10.6% has been achieved based on polymer donors and fullerene acceptors.[5] Though the great progress has been made in polymer solar cells, the batch to batch variation issue of polymers due to their intrinsic polydispersity characteristics could hinder the performance reproducibility when using polymer solar cells in commercial applications. Comparing with polymers, small molecules possess the advantages of defined molecular structure, definite molecular weight, high purity, and good reproducibility.[6,7] Recently, a variety of new small molecule donors have been created for OSCs.[8−13] To date, the highest PCEs of solution processed OSCs based on small molecule donors and fullerene acceptors are over 9%.[14,15] Despite the fact that big improvement has been made in small molecule OSCs, exploiting new molecules is needed to realize commercial applications.

As one type of push-pull structures, A-D-A type small molecules generally consist of electron-donating unit (D) as central building block, electron-accepting unit (A) as end group, and usually oligothiophene as π-conjugation bridge.[16] This type of molecule architecture can effectively tune HOMO and LUMO levels, lower band gap (E_g) and extend absorption through changing the thiophene bridge length, central building blocks and end groups. Actually, A-D-A type small molecules exhibited impressive performance in OSCs.[17−19]

As well-performed electron withdrawing units, alkyl cyanoacetate and rhodanine are introduced into A-D-A type molecules because of their capability of effectively inducing intramolecular charge transfer and enhancing optical absorp-

Received: March 5, 2014
Accepted: May 8, 2014
Published: May 8, 2014

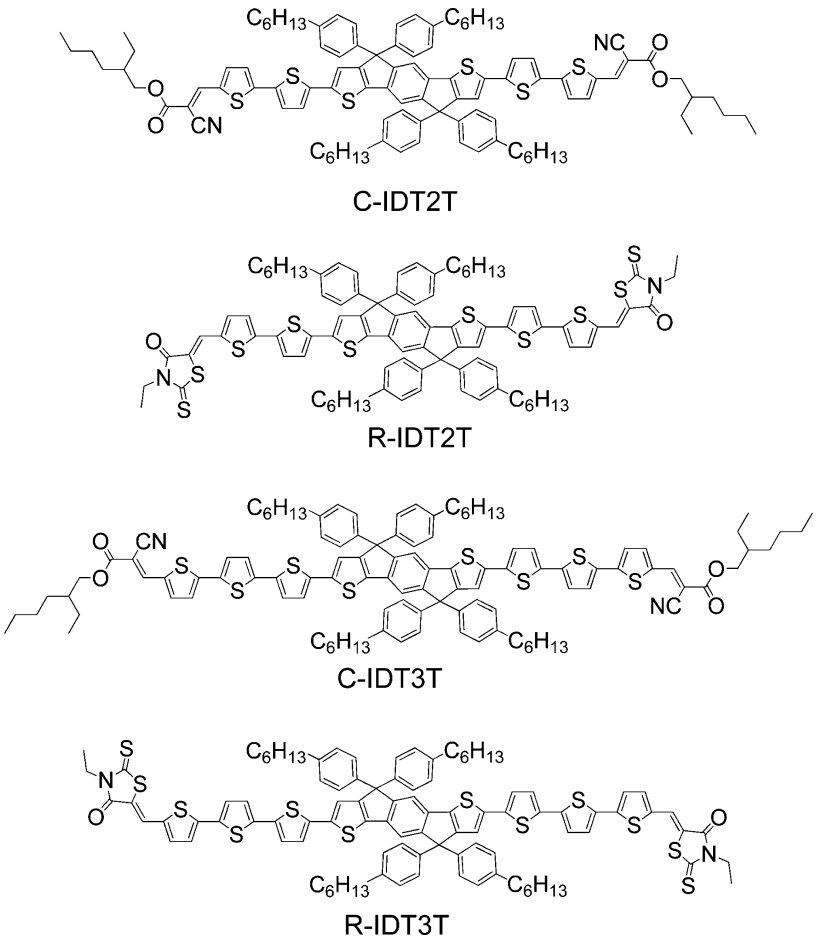

Figure 1. Chemical structure of C-IDT2T, R-IDT2T, C-IDT3T, and R-IDT3T.

Scheme 1. Synthetic Routes of C-IDT2T, R-IDT2T, C-IDT3T, and R-IDT3T

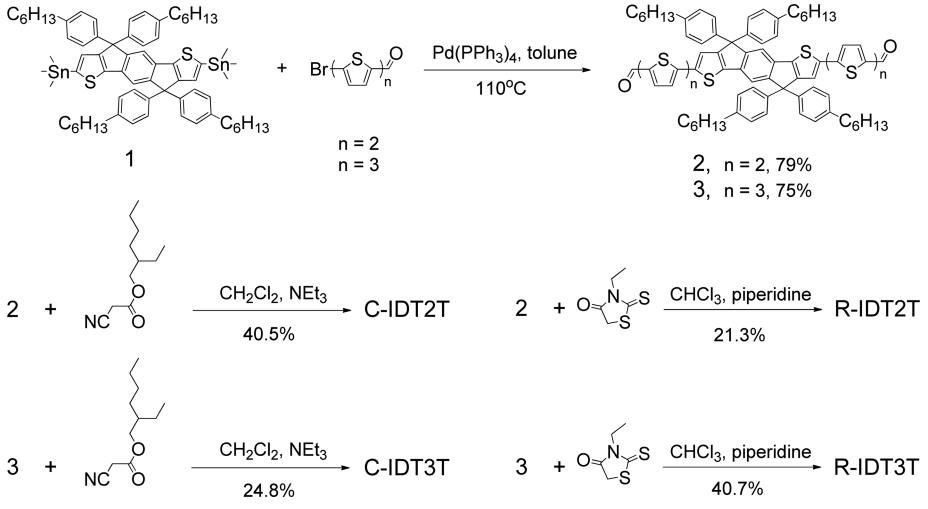

tion.[20−24] Single junction OSCs based on small molecules end-capped with alkyl cyanoacetate and rhodanine achieved the best PCEs of 5.84% and 8.12% when blending with fullerene acceptors, respectively.[25,26]

In recent years, indaceno[2,1-b:6,5-b′]dithiophene (IDT) has been regarded as a promising moiety for organic semiconductors owing to its excellent electron-donating and hole transporting property.[27−32] Due to its rigid and coplanar structure, IDT based conjugated copolymers exhibited relatively high hole mobility.[33] When applied in OSCs, IDT-based conjugated polymers showed broad absorption and high molar extinction coefficient, which is beneficial to obtaining high short circuit current (J_{SC}).[34,35] However, relative to IDT polymers, there are only a few reports on IDT small molecule photovoltaic materials, which afforded relatively low PCEs (2.8-4.7%).[36−38]

In this work, we designed and synthesized four A-D-A type small molecules, C-IDT2T, R-IDT2T, C-IDT3T and R-IDT3T

dx.doi.org/10.1021/am501316y | ACS Appl. Mater. Interfaces 2014, 6, 8426−8433

(Figure 1), using IDT unit as central donor building block, bithiophene (2T) or terthiophene (3T) as π-bridges, alkyl cyanoacetate (C) or rhodanine (R) as end acceptor groups. We investigated the effects of thiophene bridge length and end acceptor groups on absorption, energy level, charge transport, morphology and photovoltaic properties of these molecules. The OSCs based on the blends of R-IDT3T/$PC_{71}BM$ exhibited a PCE as high as 5.32%, which is the highest reported for IDT-based small molecule solar cells.

2. RESULTS AND DISCUSSION

2.1. Synthesis and Thermal Stability. The synthesis routes of these four A-D-A type small molecules are depicted in Scheme 1. The known intermediate **1** was synthesized according to the reported procedure.[39] The new intermediate compounds **2** and **3** were synthesized through Stille coupling reactions between 5′-bromo-[2,2′-bithiophene]-5-carbaldehyde or 5″-bromo-[2,2′:5′,2″-terthiophene]-5- carbaldehyde and compound **1** using $Pd(PPh_3)_4$ as catalyst. Knoevenagel condensation reactions of aldehyde compounds **2** or **3** with 2-ethylhexyl cyanoacetate or 3-ethylrhodanine afforded final products C-IDT2T, R-IDT2T, C-IDT3T and R-IDT3T. All new synthesized compounds were fully characterized by MS, ^{1}H-NMR, ^{13}C-NMR, and elemental analysis. These molecules are readily soluble in common organic solvents such as dichloromethane, chloroform, and dichlorobenzene at room temperature.

Thermal properties of these compounds were investigated by thermogravimetric analysis (TGA) and differential scanning calorimetry (DSC) methods under nitrogen atmosphere at a heating rate of 10 °C min^{-1}. All the four compounds exhibit good thermal stability with decomposition temperature (T_d, 5% weight loss) of over 360 °C in a nitrogen atmosphere (Figure 2,

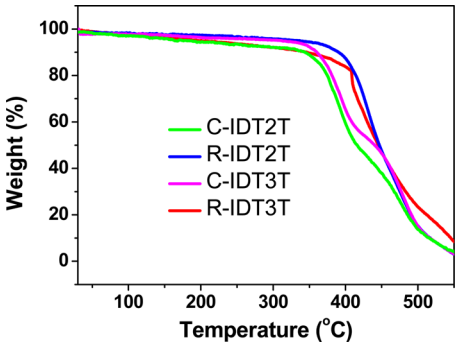

Figure 2. TGA curves of C-IDT2T, R-IDT2T, C-IDT3T, and R-IDT3T.

Table 1. Thermal and Absorption Parameters of C-IDT2T, R-IDT2T, C-IDT3T, and R-IDT3T

	T_d[a] (°C)	$\lambda_{s,max}$[b] (nm)	$\lambda_{f,max}$[c] (nm)	ε_{max}[d] (M^{-1} cm^{-1})
C-IDT2T	364	546	540	1.1×10^5
R-IDT2T	401	554	550	1.1×10^5
C-IDT3T	364	534	520	1.6×10^5
R-IDT3T	406	536	536	1.3×10^5

[a]Decomposition temperature (5% weight loss) estimated using TGA under N_2. [b]Absorption maxima in $CHCl_3$ solution. [c]Absorption maxima in film. [d]Molar extinction coefficient at λ_{max} in solution.

Table 1). According to the DSC traces (see Figure S1, in Supporting Information), R-IDT2T and R-IDT3T show glass transition at ca. 120 °C, whereas C-IDT2T and C-IDT3T show glass transition at ca. 80 °C. None of them shows melting peaks from room temperature to 250 °C, indicating that they could be amorphous.

2.2. Absorption. The normalized spectra of optical absorption of these four compounds in chloroform solution (10^{-6} M) and in solid film are shown in Figure 3. Benefited

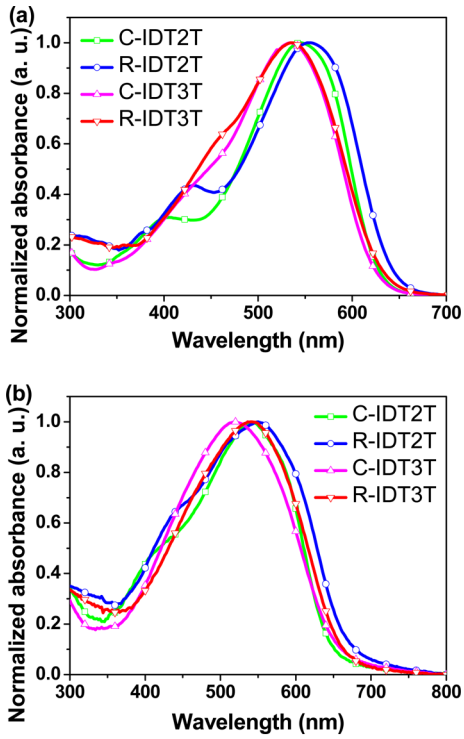

Figure 3. UV−vis absorption spectra of C-IDT2T, R-IDT2T, C-IDT3T, and R-IDT3T (a) in chloroform solution and (b) in thin films.

from their push-pull molecule structure, all the four compounds exhibit broad absorption from 400 to 650 nm in chloroform solution and solid films. C-IDT2T, R-IDT2T, C-IDT3T, and R-IDT3T exhibit absorption maxima at 546, 554, 534, 536 nm in solutions, respectively. The absorption maxima of rhodanine-containing compounds exhibit slight red shift (2−8 nm) relative to their cyanoacetate counterparts. Extending π-bridge from bithiophene to terthiophene leads to blue shift (12−18 nm) of the absorption maxima and slightly enhanced absorption intensity. Although the absorption maxima in film slightly blue shift in comparison with those in solution, all absorption spectra in films are broadened relative to those in solution.

2.3. Electrochemistry. The electrochemical property of C-IDT2T, R-IDT2T, C-IDT3T, and R-IDT3T was investigated by cyclic voltammetry (CV) method with the film on glassy carbon as working electrodes in acetonitrile solution containing 0.1 mol/L Bu_4NPF_6 at a potential scan rate of 100 mV s^{-1}. As shown in the cyclic voltammograms (see Figure S2 in the Supporting Information), these compounds exhibit irreversible reduction waves and oxidation waves. The HOMO and LUMO values of these compounds are estimated from the onset oxidation and reduction potentials, assuming the absolute energy level of $FeCp_2^{+/0}$ to be 4.8 eV below vacuum. All

dx.doi.org/10.1021/am501316y | ACS Appl. Mater. Interfaces 2014, 6, 8426−8433

compounds exhibit similar HOMO (−5.18 to −5.22 eV) and similar LUMO energies (−3.27 to −3.29 eV) (Table 2),

Table 2. CV Data and Energy Level Parameters of C-IDT2T, R-IDT2T, C-IDT3T, and R-IDT3T

	E_{ox}[a] (eV)	E_{red}[b] (eV)	HOMO[c] (eV)	LUMO[d] (eV)	E_g^{cve} (eV)	E_g^{optf} (eV)
C-IDT2T	0.88	−1.06	−5.22	−3.28	1.94	1.92
R-IDT2T	0.87	−1.07	−5.21	−3.27	1.94	1.86
C-IDT3T	0.84	−1.05	−5.18	−3.29	1.89	1.90
R-IDT3T	0.85	−1.07	−5.19	−3.27	1.92	1.88

[a]Onset oxidation potential. [b]Onset reduction potential. [c]Estimated from the onset oxidation potential. [d]Estimated from the onset reduction potential. [e]HOMO−LUMO energy gap estimated from cyclic voltammetry method. [f]Optical bandgap estimated from absorption edge of solid film.

indicating that the π-bridge length and end acceptor groups exert very limited impacts on HOMO and LUMO levels. The HOMO−LUMO energy gaps (1.89−1.94 eV) estimated from cyclic voltammetry are similar to the optical bandgaps (1.86−1.92 eV) estimated from absorption edge of solid films. As shown in Figure 4, the LUMO gaps (0.71 to 0.73 eV) and

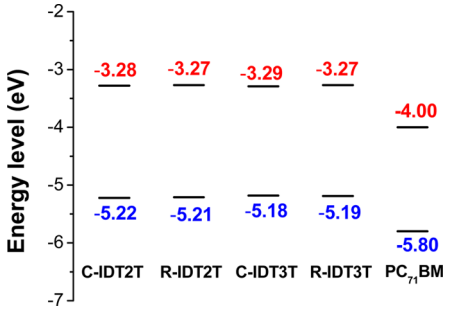

Figure 4. Electronic energy level diagram of C-IDT2T, R-IDT2T, C-IDT3T, R-IDT3T, and $PC_{71}BM$.[40]

HOMO gaps (0.58 to 0.62 eV) between the donor and acceptor ($PC_{71}BM$) are large enough to guarantee efficient exciton dissociation. The relatively low HOMO levels of these compounds are beneficial to gaining high open circuit voltage (V_{oc}) in OSCs.

2.4. Photovoltaic Properties. To demonstrate potential applications of these materials in OSCs, we used C-IDT2T, R-IDT2T, C-IDT3T and R-IDT3T as donor materials and classical fullerene derivative $PC_{71}BM$ as an electron acceptor to fabricate BHJ OSCs with a structure ITO/PEDOT:PSS/donor:$PC_{71}BM$/Ca/Al. Table 3 summarizes V_{oc}, J_{sc}, fill factor (FF), and PCE of the devices at different donor/acceptor weight ratios with or without thermal annealing. Figure 5 shows the J−V (a) curves and IPCE (b) characteristics of the four annealed devices.

After optimization, C-IDT2T-, R-IDT2T-, and C-IDT3T-based devices exhibit the best performance at the donor/acceptor weight ratio of 1:2, and R-IDT3T-based devices exhibit the best performance at the ratio of 1:3 after thermal annealing at 120 °C for 10 min. These devices yield relatively high average V_{oc} (0.87−0.93 V), which can be attributed to the relatively low HOMOs of the molecules, and the V_{oc} values are slightly affected by π-bridge length and acceptor end groups. However, when extending π-bridges from bithiophene to

Table 3. Device Data of OSCs Based on C-IDT2T, R-IDT2T, C-IDT3T, and R-IDT3T :$PC_{71}BM$ under the Illumination of AM 1.5G, 100 mW cm^{-2}

blend	donor:$PC_{71}BM$ (w/w)	V_{oc} (V)[a]	J_{sc} (mA cm^{-2})[a]	FF (%)[a]	PCE (%) ave[a]	PCE (%) best
C-IDT2T	1:2	0.87	7.96	32.8	2.27	2.40
C-IDT2T[b]	1:2	0.88	7.98	33.1	2.32	2.53
R-IDT2T	1:2	0.93	9.30	41.2	3.56	3.89
R-IDT2T[b]	1:2	0.93	10.11	44.5	4.18	4.38
C-IDT3T	1:2	0.91	10.55	45.7	4.39	4.73
C-IDT3T[b]	1:2	0.91	10.52	49.6	4.75	5.00
R-IDT3T	1:3	0.90	10.75	44.9	4.34	4.60
R-IDT3T[b]	1:3	0.90	11.55	49.0	5.09	5.32

[a]The data were obtained from 20 devices. [b]Annealing at 120 °C for 10 min.

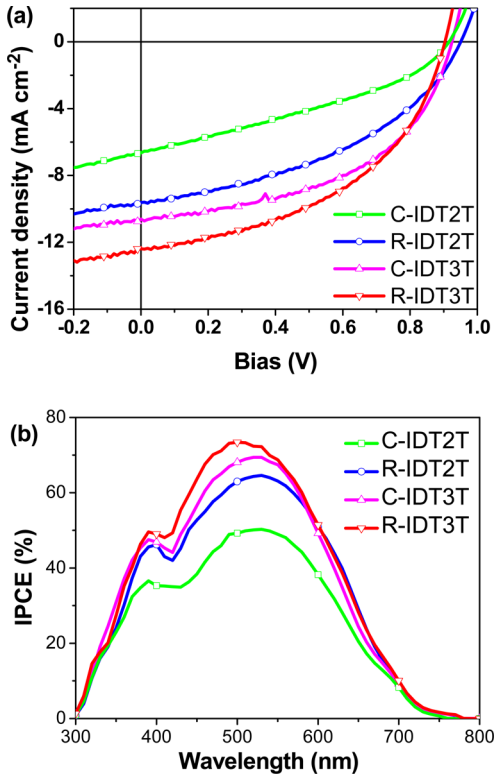

Figure 5. (a) J−V characteristics and (b) IPCE spectra of the annealed OSCs based on C-IDT2T, R-IDT2T, C-IDT3T, and R-IDT3T:$PC_{71}BM$ under the illumination of AM 1.5G, 100 mW cm^{-2}.

terthiophene, average J_{sc} increases from 7.98 (C-IDT2T) to 10.52 mA cm^{-2} (C-IDT3T) for cyanoacetate-containing compounds, and from 10.11 (R-IDT2T) to 11.55 mA cm^{-2} (R-IDT3T) for rhodanine-containing compounds. As shown in Figure 5b, the trend of IPCE is similar to that of J_{SC}. The J_{SC} calculated from integration of the IPCE spectra with the AM 1.5G reference spectrum is similar to that obtained from J−V measurement (the average error is 6%).

To understand the influence of charge carrier transport on photovoltaic performances, we measured hole and electron mobilities of four annealed blend films of C-IDT2T, R-IDT2T, C-IDT3T, and R-IDT3T:$PC_{71}BM$ by space charge limited current (SCLC) method with the device structure ITO/PEDOT:PSS/blend film/Au for holes and Al/blend film/Al for

dx.doi.org/10.1021/am501316y | ACS Appl. Mater. Interfaces 2014, 6, 8426−8433

Table 4. SCLC Data of Hole-Only and Electron-Only Devices Based on C-IDT2T, R-IDT2T, C-IDT3T, and R-IDT3T:$PC_{71}BM$ Blends

blend	donor:$PC_{71}BM$ (w/w)	annealing[a] (°C)	μ_h (cm^2 V^{-1} s^{-1})	μ_e (cm^2 V^{-1} s^{-1})
C-IDT2T:$PC_{71}BM$	1:2	120	7.5×10^{-5}	8.9×10^{-5}
R-IDT2T:$PC_{71}BM$	1:2	120	5.0×10^{-5}	2.3×10^{-5}
C-IDT3T:$PC_{71}BM$	1:2	120	1.7×10^{-4}	1.3×10^{-5}
R-IDT3T:$PC_{71}BM$	1:3	120	3.0×10^{-4}	2.7×10^{-5}

[a]Annealing for 10 min.

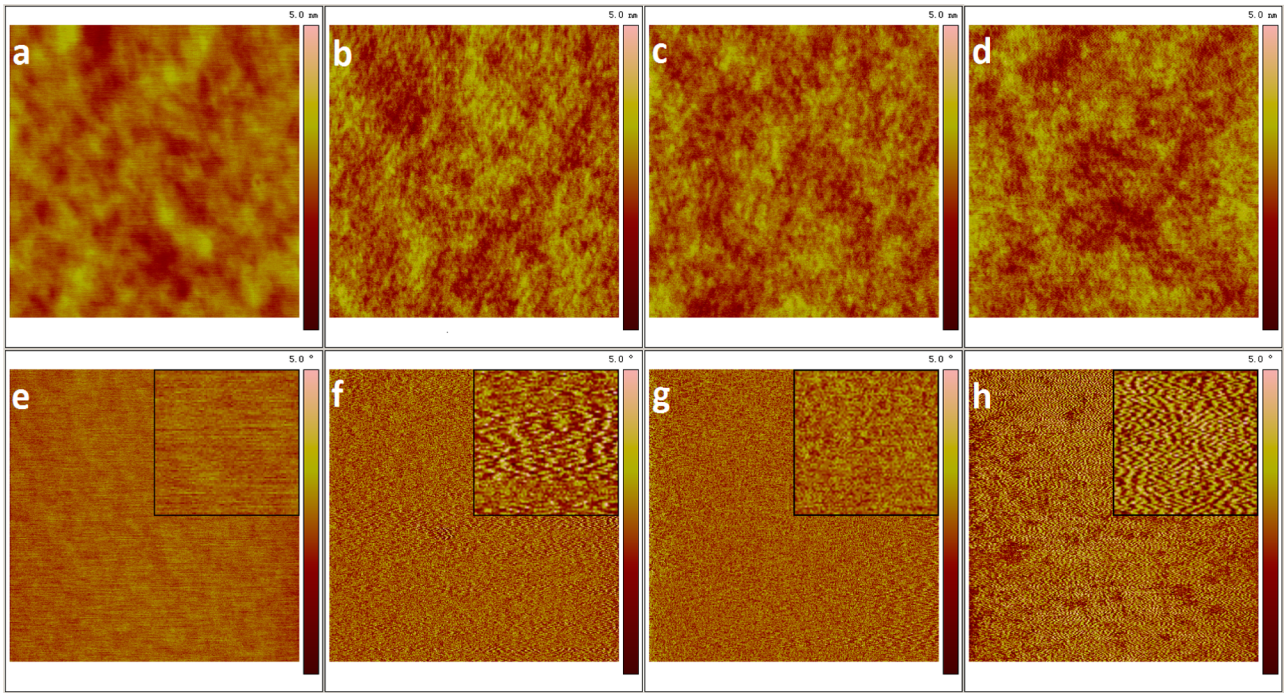

Figure 6. AFM height (top) and phase (bottom, inset 0.5 μm × 0.5 μm) images (3 μm × 3 μm) of (a, e) C-IDT2T:$PC_{71}BM$ (1:2, w/w); (b, f) R-IDT2T:$PC_{71}BM$ (1:2, w/w); (c, g) C-IDT3T:$PC_{71}BM$ (1:2, w/w); (d, h) R-IDT3T:$PC_{71}BM$ (1:3, w/w) blend films after thermal annealing at 120 °C for 10 min.

electrons (see the Supporting information, Figure S3). The detailed parameters are recorded in Table 4. After thermal annealing at 120 °C for 10 min, hole mobilities of 5×10^{-5} to 3×10^{-4} cm^2 V^{-1} s^{-1} and electron mobilities of 1.3×10^{-5} to 8.9×10^{-5} cm^2 V^{-1} s^{-1} are obtained from the four blend films (Table 4). The hole mobilities of C-IDT3T:$PC_{71}BM$ and R-IDT3T:$PC_{71}BM$ blend films are 2 and 6 times of those of C-IDT2T:$PC_{71}BM$ and R-IDT2T:$PC_{71}BM$ blend films, respectively. Clearly, extending π-bridges from bithiophene to terthiophene enhances hole transport of the molecules, which is responsible for improved J_{sc} of OSC devices.

Atomic force microscope (AFM) tapping-mode height and phase images of as-cast and annealed donor:$PC_{71}BM$ blend films are shown in Figure S4 (see the Supporting Information) and Figure 6. All the donor:$PC_{71}BM$ blend films exhibit smooth and uniform surface before and after thermal annealing in the height images. The root-mean-square (RMS) roughness of C-IDT2T, R-IDT2T, C-IDT3T, and R-IDT3T:$PC_{71}BM$ blend films are 0.317, 0.416, 0.390, and 0.428 nm, respectively. The AFM result implies that all the molecules have good miscibility with $PC_{71}BM$. In phase images, rhodanine-containing donor (R-IDT2T or R-IDT3T):$PC_{71}BM$ blend film exhibits a better donor/acceptor interpenetrating network with larger aggregated domains than its cyanoacetate counterpart (C-IDT2T or C-IDT3T:$PC_{71}BM$). The result is also supported by the transmission electron microscopy (TEM) images (see Figure S5 in the Supporting Information). Terthiophene-containing donor (C-IDT3T or R-IDT3T):$PC_{71}BM$ blend film exhibits a better donor/acceptor interpenetrating network with larger aggregated domains than its bithiophene counterpart (C-IDT2T or R-IDT2T:$PC_{71}BM$). In particular, R-IDT3T:$PC_{71}BM$ blend film exhibits best donor/acceptor interpenetrating network with largest aggregated domain size. The phase separation profile resembles the PCE profile since the suitable morphology is beneficial to the exciton dissociation and charge carriers transport, leading to improved PCE.

3. CONCLUSIONS

New series of IDT based A-D-A type small molecules with different acceptor end groups (cyanoacetate and rhodanine) and different π-bridge length (bithiophene and terthiophene), C-IDT2T, R-IDT2T, C-IDT3T, and R-IDT3T, are designed and synthesized. These molecules exhibit relatively low HOMO levels as well as strong and broad optical absorption. Both acceptor end groups and π-bridge length slightly affect absorption and energy levels of the molecules. Extending π-bridges from bithiophene to terthiophene promotes hole mobility. Both acceptor end groups and π-bridge length obviously affect nanostructure of the blend films; rhodanine or terthiophene-containing donor:$PC_{71}BM$ blend film exhibits a

better donor/acceptor interpenetrating network with larger aggregated domains than its cyanoacetate or bithiophene counterpart. In particular, R-IDT3T:$PC_{71}BM$ blend film exhibits the best phase separation and highest hole mobility, leading to the highest PCE of 5.32% after thermal annealing.

4. EXPERIMENTAL SECTION

Synthesis. Unless stated otherwise, solvents and chemicals were obtained commercially and were used without further purification. Toluene was distilled from sodium-benzophenone under nitrogen prior to use.

Synthesis of Compound 2. To a three-necked round bottom flask were added compound **1** (986.4 mg, 0.8 mmol), 5′-bromo-[2, 2′-bithiophene]-5-carbaldehyde (480 mg, 1.76 mmol), and toluene (50 mL). The mixture was deoxygenated with argon for 15 min, and then $Pd(PPh_3)_4$ (100 mg, 0.086 mmol) was added. The mixture was refluxed for 24 h and then cooled to room temperature. Forty milliliters of KF (0.1 g mL^{-1}) solution was added and stirred at room temperature overnight to remove the tin impurity. Water (150 mL) was added and the mixture was extracted with $CHCl_3$ (2 × 150 mL). The organic phase was dried over anhydrous $MgSO_4$. After removing the solvent, the residue was purified by column chromatography on silica gel using petroleum ether/$CHCl_3$ (1:2) as eluent yielding a red solid (815 mg, 79%). ^{1}H-NMR (400 MHz, CD_2Cl_2): δ 9.83 (s, 2H), 7.67 (d, J = 4 Hz, 2H), 7.46 (s, 2H), 7.29 (d, J = 4 Hz, 2H), 7.24 (d, J = 4 Hz, 2H), 7.18 (m, 12H), 7.12 (d, J = 8 Hz, 8H), 2.57 (m, 8H), 1.58 (m, 8H), 1.32 (m, 24H), 0.87 (m, 12H). ^{13}C-NMR (150 MHz, $CDCl_3$): δ 182.51, 157.11, 153.83, 146.99, 141.99, 141.77, 141.70, 141.36, 140.16, 139.18, 137.57, 135.39, 134.40, 128.73, 128.13, 127.17, 124.32, 124.16, 120.57, 117.66, 63.37, 35.83, 31.97, 31.58, 29.39, 22.85, 14.35. MS (MALDI-TOF): m/z 1292 (M^+). Anal. Calcd for $C_{82}H_{82}O_2S_6$: C, 76.16; H, 6.34. Found: C, 76.20; H, 6.35%.

Synthesis of Compound 3. To a three-necked round bottom flask were added compound **1** (986.4 mg, 0.8 mmol), 5″-bromo-[2,2′:5′,2″-terthiophene]-5-carbaldehyde (624 mg, 1.76 mmol) and toluene (50 mL). The mixture was deoxygenated with argon for 15 min, and then $Pd(PPh_3)_4$ (100 mg, 0.086 mmol) was added. The mixture was refluxed for 24 h and then cooled to room temperature. Forty milliliters of KF (0.1 g mL^{-1}) solution was added and stirred at room temperature overnight to remove the tin impurity. Water (150 mL) was added and the mixture was extracted with $CHCl_3$ (2 × 150 mL). The organic phase was dried over anhydrous $MgSO_4$. After removing the solvent, the residue was purified by column chromatography on silica gel using petroleum ether/$CHCl_3$ (1:2) as eluent yielding a red solid (873.6 mg, 75%). ^{1}H-NMR (400 MHz, CD_2Cl_2): δ 9.83 (s, 2H), 7.67 (d, J = 4 Hz, 2H), 7.46 (s, 2H), 7.29 (d, J = 4 Hz, 2H), 7.26 (d, J = 4 Hz, 2H), 7.21 (m, 8H), 7.12 (m, 16H), 2.57 (m, 8H), 1.58 (m, 8H), 1.32 (m, 24H), 0.87 (m, 12H). ^{13}C-NMR (150 MHz, $CDCl_3$): δ 182.52, 156.99, 153.73, 146.89, 141.93, 141.81, 140.86, 139.51, 139.06, 138.30, 137.54, 135.37, 134.99, 134.70, 129.08, 128.71, 128.15, 127.21, 125.36, 124.67, 124.25, 124.15, 120.11, 117.56, 63.35, 35.83, 31.97, 31.59, 29.40, 22.85, 14.35. MS (MALDI-TOF): m/z 1456 (M^+). Anal. Calcd for $C_{90}H_{86}O_2S_8$: C, 74.17; H, 5.9. Found: C, 74.40; H, 6.07%.

Synthesis of C-IDT2T. Compound **2** (320 mg, 0.247 mmol) was dissolved in dry CH_2Cl_2 (25 mL), three drops of triethylamine and then 2-ethylhexyl cyanoacetate (1.2 mL, 6 mmol) were added. The mixture was deoxygenated with argon for 15 min and stirred for 12 h under argon at room temperature. Water (100 mL) was added and the mixture was extracted with CH_2Cl_2 (2 × 100 mL). The organic phase was dried over anhydrous $MgSO_4$. After removing the solvent, the residue was purified by column chromatography on silica gel using petroleum ether/$CHCl_3$ (1:1) as eluent yielding a red black solid (165 mg, 40.5%). ^{1}H-NMR (400 MHz, CD_2Cl_2): δ 8.24 (s, 2H), 7.67 (d, J = 4 Hz, 2H), 7.46 (s, 2H), 7.34 (d, J = 4 Hz, 2H), 7.26 (s, 2H), 7.19 (m, 20H), 4.21 (m, 4H), 2.59 (m, 8H), 1.70 (m, 2H), 1.59 (m, 8H), 1.44 (m, 4H), 1.30 (m, 36H), 0.93 (m, 24H). ^{13}C-NMR (150 MHz, $CDCl_3$): δ 163.19, 156.98, 153.64, 147.11, 145.95, 141.79, 141.65, 141.47, 141.33, 140.37, 139.21, 138.94, 135.21, 134.22, 133.89, 128.53, 127.91, 127.38, 124.28, 124.16, 120.52, 117.49, 116.01, 97.63, 68.82, 63.14, 38.83, 35.63, 31.77, 31.40, 30.37, 29.20, 28.97, 23.81, 23.00, 22.65, 14.16, 11.07. MS (MALDI-TOF): m/z 1650 (M^+). Anal. Calcd for $C_{104}H_{116}N_2O_4S_6$: C, 75.68; H, 7.08; N, 1.70. Found: C, 75.48; H, 7.08; N, 1.49%. $\lambda_{max,\ s}$ = 544 nm (1.1 × 10^5 L mol^{-1} cm^{-1}).

Synthesis of R-IDT2T. Compound **2** (320 mg, 0.247 mmol) was dissolved in dry $CHCl_3$ (25 mL), and three drops of piperidine and then 3-ethylrhodanine (434.7 mg, 2.7 mmol) were added. The mixture was deoxygenated with argon for 15 min, and then refluxed and stirred for 12 h under argon. After cooling to room temperature, water (100 mL) was added and the mixture was extracted with $CHCl_3$ (2 × 100 mL). The organic phase was dried over anhydrous $MgSO_4$. After removing the solvent, the residue was purified by column chromatography on silica gel using petroleum ether/$CHCl_3$ (1:1) as eluent yielding a red black solid (83 mg, 21.3%). ^{1}H-NMR (400 MHz, CD_2Cl_2): δ 7.82 (s, 2H), 7.46 (s, 2H), 7.36 (d, J = 4 Hz, 2H), 7.26 (d, J = 4 Hz, 4H), 7.20 (m, 10H), 7.12 (d, 10H), 4.18 (m, 4H), 2.59 (m, 8H), 1.62 (m, 8H), 1.30 (m, 24H), 0.87 (m, 18H). ^{13}C-NMR (150 MHz, $CDCl_3$): δ 192.06, 167.51, 157.19, 153.85, 145.35, 142.02, 141.76, 141.37, 139.67, 136.73, 135.56, 135.46, 134.59, 128.76, 128.18, 126.48, 125.13, 125.00, 124.45, 120.80, 120.53, 117.68, 63.38, 40.21, 35.88, 32.01, 31.63, 30.00, 29.45, 22.89, 14.39, 12.57. MS (MALDI-TOF): m/z 1778 (M^+). Anal. Calcd for $C_{92}H_{92}N_2O_2S_{10}$: C, 70.01; H, 5.88; N, 1.77. Found: C, 70.15; H, 6.17; N, 1.78%. $\lambda_{max,\ s}$ = 554 nm (1.1 × 10^5 L mol^{-1} cm^{-1}).

Synthesis of C-IDT3T. Compound **3** (440 mg, 0.3 mmol) was dissolved in dry CH_2Cl_2 (25 mL), and three drops of triethylamine and then 2-ethylhexyl cyanoacetate (2 mL, 9.6 mmol) were added. The mixture was deoxygenated with argon for 15 min and stirred for 12 h under argon at room temperature. Water (100 mL) was added and the mixture was extracted with CH_2Cl_2 (2 × 100 mL). The organic phase was dried over anhydrous $MgSO_4$. After removing the solvent, the residue was purified by column chromatography on silica gel using petroleum ether/$CHCl_3$ (1:1) as eluent yielding a red black solid (135 mg, 24.8%). ^{1}H-NMR (400 MHz, CD_2Cl_2): δ 8.24 (s, 2H), 7.68 (d, J = 4 Hz, 2H), 7.45 (s, 2H), 7.34 (d, J = 4 Hz, 2H), 7.27 (s, 2H), 7.20 (m, 24H), 4.21 (m, 4H), 2.59 (m, 8H), 1.73 (m, 2H), 1.58 (m, 8H), 1.46 (m, 4H), 1.30 (m, 36H), 0.94 (m, 24H). ^{13}C-NMR (150 MHz, $CDCl_3$): δ 163.12, 156.86, 153.55, 146.96, 145.89, 141.72, 141.59, 140.75, 139.12, 138.21, 135.19, 134.81, 134.32, 128.49, 127.94, 127.37, 125.26, 124.69, 124.27, 124.07, 119.92, 117.32, 115.96, 97.75, 68.84, 63.10, 38.83, 35.62, 31.76, 31.38, 30.36, 29.74, 29.19, 29.07, 28.96, 23.81, 22.99, 22.64, 14.14, 14.09, 11.06. MS (MALDI-TOF): m/z 1814 (M^+). Anal. Calcd for $C_{112}H_{120}N_2O_4S_8$: C, 74.13; H, 6.67; N, 1.54. Found: C, 74.02; H, 6.82; N, 1.64%. $\lambda_{max,\ s}$ = 532 nm (1.6 × 10^5 L mol^{-1} cm^{-1}).

Synthesis of R-IDT3T. Compound **3** (145.6 mg, 0.1 mmol) was dissolved in dry $CHCl_3$ (25 mL), three drops of piperidine and then 3-ethylrhodanine (177 mg, 1.1 mmol) were added. The mixture was deoxygenated with argon for 15 min, and then refluxed and stirred for 12 h under argon. After cooling to room temperature, water (100 mL) was added and the mixture was extracted with $CHCl_3$ (2 × 100 mL). The organic phase was dried over anhydrous $MgSO_4$. After removing the solvent, the residue was purified by column chromatography on silica gel using petroleum ether/$CHCl_3$ (1:2) as eluent yielding a red black solid (71 mg, 40.7%). ^{1}H-NMR (400 MHz, CD_2Cl_2): δ 7.82 (s, 2H), 7.45 (s, 2H), 7.36 (d, J = 4 Hz, 2H), 7.26 (d, J = 4 Hz, 4H), 7.20 (d, J = 8 Hz, 8H), 7.14 (m, 16H), 4.18 (m, 4H), 2.59 (m, 8H), 1.62 (m, 8H), 1.30 (m, 24H), 0.87 (m, 18H). ^{13}C-NMR (150 MHz, $CDCl_3$): δ 191.90, 167.34, 156.87, 153.58, 145.09, 141.80, 141.70, 140.77, 139.36, 138.40, 138.11, 136.67, 135.36, 134.74, 131.00, 128.58, 128.04, 126.36, 125.13, 124.94, 124.64, 124.07, 120.71, 120.00, 117.43, 63.21, 40.05, 35.72, 31.86, 31.48, 29.84, 29.29, 22.73, 14.23, 12.41. MS (MALDI-TOF): m/z 1742 (M^+). Anal. Calcd for $C_{100}H_{96}N_2O_2S_{12}$: C, 68.92; H, 5.55; N, 1.61. Found: C, 68.83; H, 5.68; N, 1.71%. $\lambda_{max,\ s}$ = 540 nm (1.3 × 10^5 L mol^{-1} cm^{-1}).

Fabrication and Characterization of Photovoltaic Cells. Organic solar cells were fabricated with the structure: ITO/PEDOT:PSS/donor: $PC_{71}BM$/Ca/Al. The patterned indium tin oxide (ITO) glass (sheet resistance = 15Ω $\square^{-1}$) was pre-cleaned in an ultrasonic

bath of acetone and isopropanol, and treated in ultraviolet-ozone chamber (Jelight Company, USA) for 23 min. A thin layer (35 nm) of poly(3,4-ethylenedioxythiophene):poly(styrenesulfonate) (PEDOT: PSS, Baytron PVP AI 4083, Germany) was spin-coated onto the ITO glass and baked at 150 °C for 20 min. Donor material: $PC_{71}BM$ (30 mg mL^{-1} in total) in *o*-dichlorobenzene solvent was spin-coated on PEDOT: PSS layer to form a photosensitive layer. Thermal annealing was used after spin-coating active layer. A calcium (ca. 20 nm) and aluminum layer (ca. 100 nm) was then evaporated onto the surface of the photosensitive layer under vacuum (ca. 10^{-5} Pa) to form the negative electrode. The active area of the device was 4 mm^2. *J*–*V* curve was measured with a computer-controlled Keithley 236 Source Measure Unit. A xenon lamp coupled with AM 1.5G solar spectrum filters was used as the light source, and the optical power at the sample was 100 mW cm^{-2}. The light intensity of solar simulator was calibrated by using a standard monocrystalline silicon solar cell. The incident photon to converted current efficiency (IPCE) spectrum was measured by Stanford Research Systems model SR830 DSP lock-in amplifier coupled with WDG3 monochromator and 500 W xenon lamp. Hole-only or electron-only diodes were fabricated using the architectures: ITO/PEDOT: PSS/active layer/Au for holes and Al/active layer/Al for electrons. Mobilities were extracted by fitting the current density–voltage curves using the Mott–Gurney relationship (space charge limited current). The transmission electron microscopy (TEM) characterization was carried out on JEM-1011. The samples for the TEM measurements were prepared as follows: The active-layer films were spin-casted on ITO/PEDOT: PSS substrates, and the ITO glass with the active layers were submerged in deionized water to make the active layers float onto the air–water interface. Then the floated films were picked up on unsupported 200 mesh copper grids for the TEM measurement.

■ ASSOCIATED CONTENT

Ⓢ Supporting Information

DSC, cyclic voltammogram, SCLC figures, AFM images of as-cast films, TEM images, ^{1}H-NMR and ^{13}C-NMR spectra. These materials are available free of charge via the Internet at http://pubs.acs.org.

■ AUTHOR INFORMATION

Corresponding Author

*E-mail: xwzhan@pku.edu.cn.

Author Contributions

H.B. and Y.W. contributed equally to this paper: H.B. was responsible for the materials synthesis, whereas Y.W. was responsible for the device fabrication.

Notes

The authors declare no competing financial interest.

■ ACKNOWLEDGMENTS

We thank the NSFC (21025418, 51261130582), the 973 Program (2011CB808401), and the Chinese Academy of Sciences for financial support.

■ REFERENCES

(1) Chen, J.; Cao, Y. Development of Novel Conjugated Donor Polymers for High-Efficiency Bulk-Heterojunction Photovoltaic Devices. *Acc. Chem. Res.* **2009**, *42*, 1709–1718.

(2) Cheng, Y.-J.; Yang, S.-H.; Hsu, C.-S. Synthesis of Conjugated Polymers for Organic Solar Cell Applications. *Chem. Rev.* **2009**, *109*, 5868–5923.

(3) Li, G.; Zhu, R.; Yang, Y. Polymer Solar Cells. *Nat. Photonics* **2012**, *6*, 153–161.

(4) Li, Y. Molecular Design of Photovoltaic Materials for Polymer Solar Cells: Toward Suitable Electronic Energy Levels and Broad Absorption. *Acc. Chem. Res.* **2012**, *45*, 723–733.

(5) You, J.; Dou, L.; Yoshimura, K.; Kato, T.; Ohya, K.; Moriarty, T.; Emery, K.; Chen, C.-C.; Gao, J.; Li, G.; Yang, Y. A Polymer Tandem Solar Cell with 10.6% Power Conversion Efficiency. *Nat. Commun.* **2013**, *4*, 1446.

(6) Lin, Y.; Li, Y.; Zhan, X. Small Molecule Semiconductors for High-Efficiency Organic Photovoltaics. *Chem. Soc. Rev.* **2012**, *41*, 4245–4272.

(7) Chen, Y.; Wan, X.; Long, G. High Performance Photovoltaic Applications Using Solution-Processed Small Molecules. *Acc. Chem. Res.* **2013**, *46*, 2645–2655.

(8) Shang, H.; Fan, H.; Liu, Y.; Hu, W.; Li, Y.; Zhan, X. A Solution-Processable Star-Shaped Molecule for High-Performance Organic Solar Cells. *Adv. Mater.* **2011**, *23*, 1554–1557.

(9) Shi, Q.; Cheng, P.; Li, Y.; Zhan, X. A Solution Processable D-A-D Molecule based on Thiazolothiazole for High Performance Organic Solar Cells. *Adv. Energy Mater.* **2012**, *2*, 63–67.

(10) Bura, T.; Leclerc, N.; Bechara, R.; Lévêque, P.; Heiser, T.; Ziessel, R. Triazatruxene-Diketopyrrolopyrrole Dumbbell-Shaped Molecules as Photoactive Electron Donor for High-Efficiency Solution Processed Organic Solar Cells. *Adv. Energy Mater.* **2013**, *3*, 1118–1124.

(11) Liu, Y.; Yang, Y. M.; Chen, C. C.; Chen, Q.; Dou, L.; Hong, Z.; Li, G.; Yang, Y. Solution-Processed Small Molecules Using Different Electron Linkers for High-Performance Solar Cells. *Adv. Mater.* **2013**, *25*, 4657–4662.

(12) Sun, Y.; Welch, G. C.; Leong, W. L.; Takacs, C. J.; Bazan, G. C.; Heeger, A. J. Solution-Processed Small-Molecule Solar Cells with 6.7% Efficiency. *Nat. Mater.* **2011**, *11*, 44–48.

(13) van der Poll, T. S.; Love, J. A.; Nguyen, T.-Q.; Bazan, G. C. Non-Basic High-Performance Molecules for Solution-Processed Organic Solar Cells. *Adv. Mater.* **2012**, *24*, 3646–3649.

(14) Gupta, V.; Kyaw, A. K. K.; Wang, D. H.; Chand, S.; Bazan, G. C.; Heeger, A. J. Barium: An Efficient Cathode Layer for Bulk-heterojunction Solar Cells. *Sci. Rep.* **2013**, *3*, 1965.

(15) Liu, Y.; Chen, C.-C.; Hong, Z.; Gao, J.; Yang, Y.; Zhou, H.; Dou, L.; Li, G.; Yang, Y. Solution-Processed Small-Molecule Solar Cells: Breaking the 10% Power Conversion Efficiency. *Sci. Rep.* **2013**, *3*, 3356.

(16) Lai, Y.-Y.; Yeh, J.-M.; Tsai, C.-E.; Cheng, Y.-J. Synthesis, Molecular and Photovoltaic Properties of an Indolo[3,2-b]indole-Based Acceptor–Donor–Acceptor Small Molecule. *Eur. J. Org. Chem.* **2013**, *2013*, 5076–5084.

(17) Shen, S.; Jiang, P.; He, C.; Zhang, J.; Shen, P.; Zhang, Y.; Yi, Y.; Zhang, Z.; Li, Z.; Li, Y. Solution-Processable Organic Molecule Photovoltaic Materials with Bithienyl-benzodithiophene Central Unit and Indenedione End Groups. *Chem. Mater.* **2013**, *25*, 2274–2281.

(18) Lin, Y.; Ma, L.; Li, Y.; Liu, Y.; Zhu, D.; Zhan, X. A Solution-Processable Small Molecule Based on Benzodithiophene and Diketopyrrolopyrrole for High-Performance Organic Solar Cells. *Adv. Energy Mater.* **2013**, *3*, 1166–1170.

(19) Lin, Y.; Ma, L.; Li, Y.; Liu, Y.; Zhu, D.; Zhan, X. Small-Molecule Solar Cells with Fill Factors up to 0.75 via a Layer-by-Layer Solution Process. *Adv. Energy Mater.* **2014**, *4*, 1300626.

(20) He, G.; Li, Z.; Wan, X.; Liu, Y.; Zhou, J.; Long, G.; Zhang, M.; Chen, Y. Impact of Dye End Groups on Acceptor-Donor-Acceptor Type Molecules for Solution-Processed Photovoltaic Cells. *J. Mater. Chem.* **2012**, *22*, 9173–9180.

(21) Li, Z.; He, G.; Wan, X.; Liu, Y.; Zhou, J.; Long, G.; Zuo, Y.; Zhang, M.; Chen, Y. Solution Processable Rhodanine-Based Small Molecule Organic Photovoltaic Cells with a Power Conversion Efficiency of 6.1%. *Adv. Energy Mater.* **2012**, *2*, 74–77.

(22) Liu, Y.; Wan, X.; Wang, F.; Zhou, J.; Long, G.; Tian, J.; Chen, Y. High-Performance Solar Cells using a Solution-Processed Small Molecule Containing Benzodithiophene Unit. *Adv. Mater.* **2011**, *23*, 5387–5391.

(23) Liu, Y.; Wan, X.; Wang, F.; Zhou, J.; Long, G.; Tian, J.; You, J.; Yang, Y.; Chen, Y. Spin-Coated Small Molecules for High Performance Solar Cells. *Adv. Energy Mater.* **2011**, *1*, 771–775.

(24) Zhou, J.; Wan, X.; Liu, Y.; Zuo, Y.; Li, Z.; He, G.; Long, G.; Ni, W.; Li, C.; Su, X.; Chen, Y. Small Molecules Based on Benzo[1,2-b:4,5-b′]dithiophene Unit for High-Performance Solution-Processed Organic Solar Cells. *J. Am. Chem. Soc.* **2012**, *134*, 16345−16351.
(25) Zhou, J.; Wan, X.; Liu, Y.; Long, G.; Wang, F.; Li, Z.; Zuo, Y.; Li, C.; Chen, Y. A Planar Small Molecule with Dithienosilole Core for High Efficiency Solution-Processed Organic Photovoltaic Cells. *Chem. Mater.* **2011**, *23*, 4666−4668.
(26) Zhou, J.; Zuo, Y.; Wan, X.; Long, G.; Zhang, Q.; Ni, W.; Liu, Y.; Li, Z.; He, G.; Li, C.; Kan, B.; Li, M.; Chen, Y. Solution-Processed and High-Performance Organic Solar Cells Using Small Molecules with a Benzodithiophene Unit. *J. Am. Chem. Soc.* **2013**, *135*, 8484−8487.
(27) Bronstein, H.; Leem, D. S.; Hamilton, R.; Woebkenberg, P.; King, S.; Zhang, W.; Ashraf, R. S.; Heeney, M.; Anthopoulos, T. D.; Mello, J. d.; McCulloch, I. Indacenodithiophene-co-benzothiadiazole Copolymers for High Performance Solar Cells or Transistors via Alkyl Chain Optimization. *Macromolecules* **2011**, *44*, 6649−6652.
(28) Zhang, M.; Guo, X.; Wang, X.; Wang, H.; Li, Y. Synthesis and Photovoltaic Properties of D−A Copolymers Based on Alkyl-Substituted Indacenodithiophene Donor Unit. *Chem. Mater.* **2011**, *23*, 4264−4270.
(29) Zhang, W.; Smith, J.; Watkins, S. E.; Gysel, R.; McGehee, M.; Salleo, A.; Kirkpatrick, J.; Ashraf, S.; Anthopoulos, T.; Heeney, M.; McCulloch, I. Indacenodithiophene Semiconducting Polymers for High-Performance, Air-Stable Transistors. *J. Am. Chem. Soc.* **2010**, *132*, 11437−1439.
(30) Zhang, Y.; Zou, J.; Yip, H.-L.; Chen, K.-S.; Zeigler, D. F.; Sun, Y.; Jen, A. K. Y. Indacenodithiophene and Quinoxaline-Based Conjugated Polymers for Highly Efficient Polymer Solar Cells. *Chem. Mater.* **2011**, *23*, 2289−2291.
(31) Guo, X.; Zhang, M.; Tan, J.; Zhang, S.; Huo, L.; Hu, W.; Li, Y.; Hou, J. Influence of D/A Ratio on Photovoltaic Performance of a Highly Efficient Polymer Solar Cell System. *Adv. Mater.* **2012**, *24*, 6536−6541.
(32) Yao, K.; Intemann, J. J.; Yip, H.-L.; Liang, P.-W.; Chang, C.-Y.; Zang, Y.; Li, Z. a.; Chen, Y.; Jen, A. K. Y. Efficient All Polymer Solar Cells from Layer-Evolved Processing of a Bilayer Inverted Structure. *J. Mater. Chem. C* **2014**, *2*, 416−420.
(33) Chan, S. H.; Chen, C. P.; Chao, T. C.; Ting, C.; Lin, C. S.; Ko, B. T. Synthesis, Characterization, and Photovoltaic Properties of Novel Semiconducting Polymers with Thiophene−Phenylene−Thiophene (TPT) as Coplanar Units. *Macromolecules* **2008**, *41*, 5519−5526.
(34) Chen, C.-P.; Chan, S.-H.; Chao, T.-C.; Ting, C.; Ko, B.-T. Low-Bandgap Poly(Thiophene-Phenylene-Thiophene) Derivatives with Broaden Absorption Spectra for Use in High-Performance Bulk-Heterojunction Polymer Solar Cells. *J. Am. Chem. Soc.* **2008**, *130*, 12828−12833.
(35) Yu, C.-Y.; Chen, C.-P.; Chan, S.-H.; Hwang, G.-W.; Ting, C. Thiophene/Phenylene/Thiophene-Based Low-Bandgap Conjugated Polymers for Efficient Near-Infrared Photovoltaic Applications. *Chem. Mater.* **2009**, *21*, 3262−3269.
(36) Yong, W.; Zhang, M.; Xin, X.; Li, Z.; Wu, Y.; Guo, X.; Yang, Z.; Hou, J. Solution-Processed Indacenodithiophene-Based Small Molecule for Bulk Heterojunction Solar Cells. *J. Mater. Chem. A* **2013**, *1*, 14214−14220.
(37) Bai, H.; Cheng, P.; Wang, Y.; Ma, L.; Li, Y.; Zhu, D.; Zhan, X. A Bipolar Small Molecule based on Indacenodithiophene and Diketopyrrolopyrrole for Solution Processed Organic Solar Cells. *J. Mater. Chem. A* **2014**, *2*, 778−784.
(38) Liu, X.; Li, Q.; Li, Y.; Gong, X.; Su, S.; Cao, Y. Indacenodithiophene Core-Based Small Molecules with Tunable Side Chains for Solution-Processed Bulk Heterojunction Solar Cells. *J. Mater. Chem. A* **2014**, *2*, 4004−4013.
(39) Chen, Y. C.; Yu, C. Y.; Fan, Y. L.; Hung, L. I.; Chen, C. P.; Ting, C. Low-Bandgap Conjugated Polymer for High Efficient Photovoltaic Applications. *Chem. Commun.* **2010**, *46*, 6503−6505.
(40) Walker, B.; Tamayo, A. B.; Dang, X. D.; Zalar, P.; Seo, J. H.; Garcia, A.; Tantiwiwat, M.; Nguyen, T. Q. Nanoscale Phase Separation and High Photovoltaic Efficiency in Solution-Processed, Small-Molecule Bulk Heterojunction Solar Cells. *Adv. Funct. Mater.* **2009**, *19*, 3063−3069.